ARTICLE

Laser Induced Fluorescence Spectroscopy of IrN†

H. F. Pang, A. S. C. Cheung*

Department of Chemistry, The University of Hong Kong, Pokfulam Road, Hong Kong, China

High resolution laser induced fluorescence spectra of IrN in the spectral region between 394 and 520 nm were recorded using laser vaporization/reaction free jet expansion and laser induced fluorescence spectroscopy. Seven new vibronic transition bands were observed and analyzed. Two $\Omega=1$ and five $\Omega=0$ new states were identified. Least squares fit of rotationally resolved transition lines yielded accurate molecular constants for the upper states. Spectra of isotopic molecules were observed, which provided confirmation for the vibrational assignment. Comparison of the observed electronic states of IrB, IrC, and IrN provides a good understanding of the chemical bonding of this group of molecules.

Key words: Electronic transition, Rotational analysis, Iridium mononitride, Laser induced fluorescence spectroscopy

I. INTRODUCTION

Iridium compounds are well known important catalysts in the formation of carbon-hydrogen and carbon-oxygen bonds [1,2]. Despite these important characteristics, only limited gas-phase spectroscopic studies have been performed on iridium compounds. It is important to have a good understanding of chemical bonding in a variety of iridium molecules to enhance our knowledge of its catalytic properties. The formation of chemical bond depends on the electron occupation of orbitals formed from the atoms involved, and such information is available from electronic structure. Recently, electronic and molecular structures of some diatomic molecules formed from the iridium atom and one of the first row main group elements, such as IrB, IrC, and IrN, have been investigated [3-13]. For these molecules, the ground state is generally well characterized; however, investigation of excited electronic states is still limited.

The optical spectrum of IrN was first studied by Marr *et al.* using laser induced fluorescence (LIF) spectroscopy [6,7]. The $A^1\Pi$-$X^1\Sigma^+$ transition was observed and reported, which included the rotational, fine and hyperfine constants, magnetic g_J-factor and electric dipole moment for the $A^1\Pi$ and $X^1\Sigma^+$ states. Bernath and co-workers using Fourier transform emission spectroscopy [10,11], observed electronic transitions in the visible and near infrared regions between 500 and 1300 nm. They identified two new low-lying electronic states namely: $A'^1\Pi$ and $a^3\Pi$ states in addi-

tion to the $A^1\Pi$ state. They also performed *ab initio* calculations to assist the assignment of the observed transitions.

In this work, we report the analysis of electronic transitions of IrN in the spectral region between 390 and 520 nm using laser ablation/reaction free jet expansion and LIF spectroscopy. The aim of this work is to study and characterize the excited electronic states of IrN. The observed electronic states of IrN are compared with IrB and IrC to understand the chemical bonding of this group of molecules.

II. EXPERIMENTS

The laser ablation/reaction free jet expansion setup with the LIF spectrometer has been described in a previous work [14]. Only a brief description of the relevant experimental conditions is given here. Pulses of 532 nm radiation from a Nd:YAG laser (5-6 mJ and 10 ns) were focused onto the surface of the iridium rod to obtain metal atoms. A pulsed valve was synchronized with an appropriate time delay released gas mixture of 3% NH_3 in argon to react with the iridium metal atoms for the production of IrN. The jet-cooled molecules were excited by a tunable pulsed dye laser pumped by a Nd:YAG laser. The LIF signal was collected by means of a lens system and detected by a photomultiplier tube (PMT). The PMT output was fed into a fast oscilloscope for averaging and storage. The laser linewidth of the pulsed dye laser system used in this work was about 0.06 cm^{-1}, and the laser wavelength was calibrated using an optogalvanic cell with known argon lines.
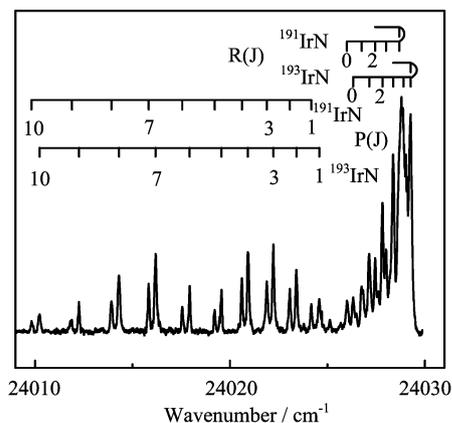
FIG. 1 High resolution spectrum of the (0, 0) band of $^1\Sigma^+$-$X^1\Sigma^+$ transition of IrN.

FIG. 2 High resolution spectrum of the (1, 0) band of $^1\Sigma^+$-$X^1\Sigma^+$ transition of IrN.
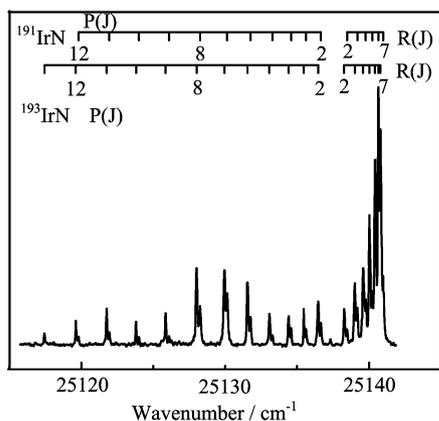

FIG. 3 High resolution spectrum of the (5, 0) band of $A^1\Pi$-$X^1\Sigma^+$ transition of IrN.

III. RESULTS AND DISCUSSION

Figure 1 shows the (0, 0) band of a new electronic transition at 24025 cm^{-1}, which has only P and R branches. Such a simple pattern characterizes a $\Omega=0 \leftarrow X^1\Sigma^+$ transition. Figure 2 depicts another similar transition at 25137 cm^{-1}. It is interesting to note the intensity of rotational lines of the two isotopes in these two bands. The abundance of the ^{191}Ir and ^{193}Ir atoms are 37.3% and 62.7% respectively, and the stronger rotational lines in the two figures belong to the ^{193}IrN molecule. Under normal circumstance, only the (0, 0) band would have the P branch lines of the ^{193}IrN molecule appeared on the higher frequency side of the ^{191}IrN lines as in Fig.1, and for other vibronic transition such as the 25137 cm^{-1} band the lines are reversed. From the isotopic shift measurement, it is reasonable to assign the 25137 cm^{-1} transition as the (1, 0) band. The ground state of IrN is $X^1\Sigma^+$, which implies the electric dipole allowed transitions that can be directly connected to it are only the $^1\Sigma^+$ and $^1\Pi$ states.
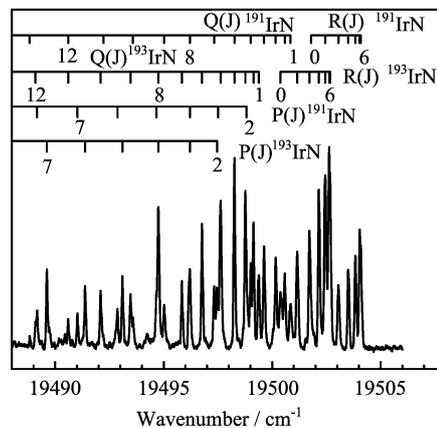
However, if the spin-orbit interaction in a molecule is strong, then the mixing of electronic wave function allows the observation of forbidden transitions such as singlet to triplet transitions. We observed five transitions with $\Omega=0$ upper states and two $\Omega=1$ states. Beranth and coworkers observed sub-band transitions between singlet and triplet: $^3\Pi$-$X^1\Sigma^+$ transition with $^3\Pi_0$-$X^1\Sigma^+$ and $^3\Pi_1$-$X^1\Sigma^+$ subbands [10]. The $\Omega=1$ sub-band observed at 22837 cm^{-1} fits quite well with the $v=5$ level $^3\Pi$-$X^1\Sigma^+$ transition detected by Beranth and it is reasonable for it to be part of a triplet state, possibly a $^3\Pi$ state, however, we have not been able to locate the related $\Omega=0$ sub-band. Another reason for the 22837 cm^{-1} band to be part of the $^3\Pi$-$X^1\Sigma^+$ transition is that, from considering specific electronic configurations, only two low-lying $^1\Pi$ states are expected and they have been accounted for [10,11]. It is not likely that other low energy electronic configuration could give rise to another low-lying $^1\Pi$ state. The isotopic shift of this level is about 1.5 cm^{-1} and it fits well with a $v=5$ level, which indicates the origin of the electronic state is below 17800 cm^{-1}. Figure 3 shows a band at 19500 cm^{-1}, with P, Q, and R branches, which was assigned as the (5, 0) band of the $A^1\Pi$-$X^1\Sigma^+$ transition. The isotopic shift of this band is about 1.4 cm^{-1}. Judging from the isotopic separation, the recorded bands are with vibrational quantum number ranging from $v=2$ up to $v=8$. The origin of these electronic states should be in the visible region. Due to the fact that only Σ^+ and Π states are reachable by the $X^1\Sigma^+$ state and some bands are quite weak, the information available is fragmented and many of the bands obtained are not classified yet. Further work is necessary for clarifying the situation. Our observed line positions of each band were fit to the following expression [15]:

$$\nu = \nu_0 + B'J'(J'+1) - D'[J'(J'+1)]^2 - \{B''J''(J''+1) - D''[J''(J''+1)]^2\} \quad (1)$$

TABLE I Molecular constants for the upper states of IrN and its isotope.

Transition	$v'-v''$	$\Delta\nu$	^{191}IrN		^{193}IrN		r'_v/Å
			ν_0/cm^{-1}	B'_v/cm^{-1}	ν_0/cm^{-1}	B'_v/cm^{-1}	
$A^1\Pi \leftarrow X^1\Sigma^+$	5-0	1.41	19500.92(2)	0.43314(29)	19499.51(2)	0.43203(22)	1.7288
$^3\Pi_1 \leftarrow X^1\Sigma^+$	5-0	1.50	22835.45(3)	0.41958(66)	22833.95(4)	0.41746(83)	1.7587
Unclassified: $\Omega=0 \leftarrow X^1\Sigma^+$	8-0	2.26	22987.12(4)	0.42080(67)	22984.86(3)	0.41939(63)	1.7547
	3-0	0.87	22165.95(4)	0.41578(92)	22165.08(4)	0.41473(79)	1.7645
	0-0	−0.32	24025.24(4)	0.44026(80)	24025.56(2)	0.43989(70)	1.7133
	1-0	0.23	25137.75(7)	0.43535(15)	25137.52(7)	0.43522(12)	1.7224
	1-0	0.29	25992.10(5)	0.42826(94)	25991.81(5)	0.42743(97)	1.7381

where the usual meaning of $'$ and $''$ are, respectively, for the upper and lower states. ν_0 is the band origin, and B and D are the rotational and centrifugal distortion constants. In the band by band least squares fit, the ground state molecular constants were held fixed to those of Marr et al. [6]. Because only relatively low J lines are measured, the centrifugal distortion constant D was set to zero. Molecular constants obtained are listed in Table I. A list of the measured line positions of ^{191}IrN and ^{193}IrN is available from the authors.

Molecular parameters of isotopic molecules are approximately related by different powers of the mass dependence parameter $\rho=\mu/\mu_i$, where μ and μ_i are the reduced mass of ^{191}IrN and its heavier isotope ^{193}IrN respectively. Since ^{193}IrN is the most abundant isotope, isotopic effects are calculated relative to it. The agreement between the two isotopic molecules is excellent.

It is legitimate to consider the main group atom as a ligand to split the iridium d orbitals. Figure 4 presents qualitatively the relative energy of the molecular orbitals (MOs) formed from iridium and the main group: B, C, and N atoms. Since the main group atom has no valence orbital with δ symmetry, the 1δ MO is essentially unaffected by the main group atom, therefore, the MOs are arranged in a way so that the 1δ MO of the main group element is placed at the same energy in the Fig.4. The molecular orbital energy level depends on the relative energy of the 5d and 6s orbitals of the Ir atom and the 2p orbital of the main group atom. The first ionization potential (IP) of Ir (880 kJ/mol) and the main group atoms (B: 800.6 kJ/mol, C: 1086.2 kJ/mol, and N: 1402.3 kJ/mol) indicates how difficult it is to remove the outermost electron, which also establishes the relative energy of the valence orbital of the Ir and the main group atoms. MOs formed from the Ir 6s and 5d atomic orbitals (AOs) and the main group atomic 2p AOs. The 1σ and 2σ MOs are, respectively, constructed from bonding and antibonding combinations of the $5d\sigma$ (Ir) and $2p\sigma$ (main group). The 2σ MO also has some of the $6s\sigma$ (Ir) and $2p\sigma$ (main group) bonding character. The 1π and 2π MOs are respectively formed from the bonding and antibonding combinations of the $5d\pi$ (Ir) and $2p\pi$ (main group). The 3σ MO is the antibonding analog of 2σ MO. The 1δ MO is essentially a pure Ir 5df
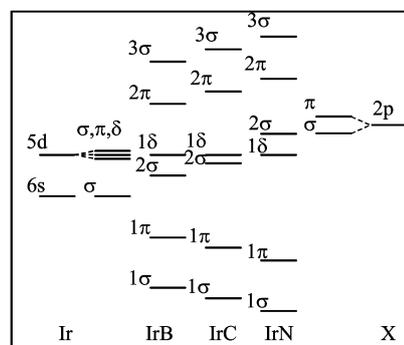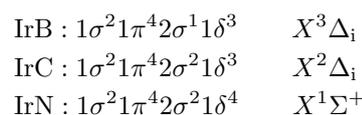

FIG. 4 Molecular orbital energy level diagram of IrX where X=B, C, and N.

AO, which is non-bonding orbital. Using a single configuration approach, the major electronic configuration giving rise to the ground state of the molecules is:

$$\text{IrB} : 1\sigma^2 1\pi^4 2\sigma^1 1\delta^3 \qquad X^3\Delta_i$$
$$\text{IrC} : 1\sigma^2 1\pi^4 2\sigma^2 1\delta^3 \qquad X^2\Delta_i$$
$$\text{IrN} : 1\sigma^2 1\pi^4 2\sigma^2 1\delta^4 \qquad X^1\Sigma^+$$

We examined further the electronic state of the IrN molecule, and the main configurations giving rise to low-lying electronic states are listed in Table II. Bernath et al. showed that the $A'^1\Pi$ and $A^1\Pi$ states arise from the promotion of 2σ MO to the 2π MO and 1δ MO to the 2π MO respectively [11], which has the configurations labeled as C and D. The $a^3\Pi$ observed is a mixture with similar contributions from the two configurations (labeled as C and D) mentioned in Table II. The many $^1\Sigma^+$ states obtained in this work can somehow be accounted for with configuration labeled as B and F, but accurate association of the configurations to the electronic states will have to wait for more work to be performed.

Table III lists the electronic states observed so far for the three molecules IrB, IrC, and IrN. They are arranged with respect to the promotion of electron from the ground state configuration to various MO. Table III compares mainly the r_0, $\Delta G_{1/2}$, and T_0 rather than the equilibrium constants, because this information is

TABLE II Electronic configurations of the low-lying electronic states of IrN.

Label	Molecular orbital occupancies						Configuration	States
	1σ	1π	2σ	1δ	2π	3σ		
A	2	4	2	4			Close shell	$X^1\Sigma^+$
B	2	4	1	4		1	$\sigma\sigma$	$^1\Sigma^+$, $^3\Sigma^+$
C	2	4	1	4	1		$\sigma\pi$	$^1\Pi$, $^3\Pi$
D	2	4	2	3	1		$\delta^3\pi$	$^3\Phi$, $^3\Pi$, $^1\Phi$, $^1\Pi$
E	2	4	2	3		1	$\delta^3\sigma$	$^1\Delta$, $^3\Delta$
F	2	3	2	4	1		$\pi^3\pi$	$^1\Sigma^+$, $^3\Sigma^+$, $^1\Sigma^-$, $^3\Sigma^-$, $^1\Delta$, $^3\Delta$
G	2	3	2	4		1	$\pi^3\sigma$	$^1\Pi$, $^3\Pi$

TABLE III Spectroscopic constants for the observed low-lying states of IrB, IrC, and IrN (energy in cm^{-1}, r_0 in Å).

Electron promotion	IrB	IrC	IrN
$2\sigma\rightarrow2\pi$		$[23.0]^2\Pi_{3/2}(2\sigma^1 1\delta^3 2\pi^1)$	$A'^1\Pi(2\sigma^1 1\delta^4 2\pi^1)$
		$T_0=23002.2^*$, $r_0=1.6603$,	$r_0=1.6786$, $\omega_e=1014.06$,
		$\Delta G_{1/2}=808^*$	$T_0=13135.39$
$2\sigma\rightarrow2\pi$	$[16.5]^3\Pi_2(1\delta^3 2\pi^1)$	$L^2\Phi_{7/2}(2\sigma^1 1\delta^3 2\pi^1)$	$a^3\Pi(2\sigma^1 1\delta^4 2\pi^1)$
	$r_0=1.8487$, $\omega_e=686.96$,	$r_0=1.7557$, $\Delta G_{1/2}=817.3$,	$r_0=1.6603$, $A=-340.53$,
	$\Delta G_{1/2}=644.84$, $T_0=16203.627$	$T_0=20816.34$	$T_0=8840.32$, $\Delta G_{1/2}=984.36$
$1\delta\rightarrow2\pi$		$[19.4]^2\Pi_{3/2}(2\sigma^2 1\delta^2 2\pi^1)$	$A^1\Pi(2\sigma^2 1\delta^3 2\pi^1)$
		$r_0=1.7130$, $T_0=19434.34$	$r_0=1.6847$, $\omega_e=936.73$, $T_0=15186.75$
		$K^2\Pi_{3/2}(2\sigma^2 1\delta^2 2\pi^1)$	
		$r_0=1.7229$, $T_0=19236.16$,	
		$\Delta G_{1/2}=833.1$, $r_0=1.7198$	
$1\delta\rightarrow2\pi$		$D^2\Phi_{7/2}(2\sigma^2 1\delta^2 2\pi^1)$	
		$r_0=1.7216$, $T_0=15277.5$,	
		$\Delta G_{1/2}=924$	
Ground state	$X^3\Delta_3(2\sigma^1 1\delta^3)$	$X^2\Delta_{5/2}(2\sigma^2 1\delta^3)$	$X^1\Sigma^+(2\sigma^2 1\delta^4)$
	$r_0=1.7675$	$r_0=1.6852$	$r_0=1.6068$

* Values obtained from calculation.

ready available. It is easily noticeable that, for the ground state, as the 2σ and 1δ MOs are approaching close shell configuration, the bond length is shortened from IrB to IrN. In fact, IrN has the shortest bond length and the strongest chemical bond with highest vibrational frequency among these three molecules. A quick observation is that for each of the molecules, all upper states have longer bond length than the respective ground state, which is reasonable because taking an electron from the bonding orbital and putting it into either non-bonding or anti-bonding orbitals would weaken the chemical bond. Table III also shows that for individual molecule with a particular electronic configuration, electronic states with larger spin multiplicity, S, or larger orbital angular momentum, Λ, are lower in energy. The situation compares well the Hund's rule for atomic states [16]. For instance in IrC, the electronic configuration: $2\sigma^1 1\delta^3 2\pi^1$, the $L^2\Phi_{7/2}$ is lower in energy than the $[23.0]^2\Pi_{3/2}$ state, and for the electronic configuration: $2\sigma^2 1\delta^2 2\pi^1$, the $D^2\Phi_{7/2}$ state is of lower

energy than the $[19.4]^2\Pi_{3/2}$ and the $K^2\Pi_{3/2}$ states. For the configuration: $2\sigma^2 1\delta^3 2\pi^1$ of IrN, the $a^3\Pi$ state is of lower energy than the $A^1\Pi$ state. Table III shows that for IrB only one transition was identified, although it is reasonable to expect that electronic transitions resulting from the promoted of an electron from the 1δ to the 2π MO should be possible and within the ultra violet and visible wavelength regions. Further work on IrB in the shorter wavelength range would be useful to better understand this molecule.

IV. CONCLUSION

This work provides an opportunity to examine the upper electronic states of IrN; it shows that the identification of electronic state is getting more and more difficult as we move up the energy scale. This is partly because the iridium atom has a very large spin-orbit parameter $\xi=3617$ cm^{-1} [17], which implies

generally that diatomic molecules involving iridium atom would be expected to have large spin-orbit interaction. Therefore, the different spin components in an electronic state are usually widely separated and only the Ω value of a sub-state can be identified but not the Λ value. In addition, there are intensity variations in a vibronic transition; it is not easy to recognize vibrational progressions. These are major reasons for many sub-bands to be listed as unclassified.

V. ACKNOWLEDGMENTS

[1] M. A. Ciriano, J. A. Lopez, L. A. Oro, J. J. Perez-torrente, M. Lanfranchi, A. Tiripicchio, and M. T. Camellini, Organometallics, **14**, 4764 (1995).
[2] R. J. Catano and M. B. Hall, Organometallics **15**, 1889 (1996).
[3] J. Ye, H. F. Pang, A. M. Y. Wong, J. W. H. Leung, and A. S. C. Cheung, J. Chem. Phys. **128**, 154321 (2008).
[4] K. Jansson, R. Scullman, and B. Yttermo, Chem. Phys. Lett. **4**, 188 (1969).
[5] K. Jansson and R. Scullman, J. Mol. Spectros. **36**, 248 (1970).
[6] A. J. Marr, M. E. Flores, and T. C. Steimle, J. Chem. Phys. **104**, 8183 (1996).
[7] H. Tan, M. Z. Liao, and K. Balasubramanian, Chem. Phys. Lett. **280**, 219 (1997).
[8] T. M. Ma, J. W. H. Leung, and A.S. C. Cheung, Chem. Phys. Lett. **385**, 259 (2004).
[9] T. C. Steimle, A. J. Marr, S. A. Beaton, and J. M. Brown, J. Chem. Phys. **106**, 2073 (1997).
[10] R. S. Ram, J. Lievin, and P. F. Bernath, J. Mol. Spectrosc. **197**, 133 (1999).
[11] R. S. Ram and P. F. Bernath, J. Mol. Spectrosc. **193**, 363 (1999).
[12] V. Raziunas, G. Macur, and S. Katz, J. Chem. Phys. **43**, 1010 (1965).
[13] K. Jansson and R. Scullman, J. Mol. Spectrosc. **43**, 208 (1972).
[14] Q. Ran, W. S. Tam, C. S. Ma, and A. S. C. Cheung, J. Mol. Spectrosc. **198**, 175 (1999).
[15] G. Herzberg, *Spectra of Diatomic Molecules*, New York: Van Nostrand, (1950).
[16] G. Herzberg, *Atomic Spectra and Atomic Structure*, New York: Dover, (1944).
[17] H. Lefebvre-Brion and R. W. Field, *The Spectra and Dynamics of Diatomic Molecules*, New York: Elsevier, (2004).